

## Phases of Helium Adsorbed on Graphite: A Feynman Path-Integral Monte Carlo Study

Farid F. Abraham

*IBM Almaden Research Center, San Jose, California 95120*

and

Jeremy Q. Broughton

*Materials Science Department, State University of New York at Stony Brook, Stony Brook, New York 11794*

(Received 23 March 1987)

The phases of  $^3\text{He}$  adsorbed on graphite are simulated by use of the Feynman path-integral Monte Carlo method. The fluid, commensurate solid, incommensurate solid, and reentrant fluid phases are found and are in agreement with the experimental phase diagram. The microscopic structure of the reentrant fluid is observed to be a striped domain-wall liquid and is consistent with a recent experimental interpretation and theoretical model. Larger-size systems are required for further quantitative analysis of the domain-wall liquid.

PACS numbers: 67.70.+n, 64.70.-p, 67.50.-b, 68.55.-a

This study was largely inspired by the beautiful phase diagram of helium on graphite which was presented by Schick<sup>1</sup> as his interpretation of experimental data, and by our desire to see if the quantum Monte Carlo method<sup>2,3</sup> could verify the diagram and give important information on the microstructure of the adsorbed phases. Schick's phase diagram is presented in Fig. 1, but we note that the  $\beta$  phase was not part of his original picture. In fact, our expectation was to find a typical high-density fluid in the  $\beta$ -phase region. Up to the present, there have been a few significant successes in the study of the quantum many-body problem at finite temperature with use of computer simulation.<sup>2,3</sup> However, we would highlight the very impressive  $^4\text{He}$  simulation of Bose-Einstein condensation by Ceperley and Pollock.<sup>5</sup> We selected  $^3\text{He}$  for our study so as to attack the Fermi-statistics problem which can plague attempts to obtain reasonable averages basic to the Monte Carlo sampling procedure. It was only after we had implemented a scheme for accounting for Fermi statistics that we learned from computer experimentation that exchange was not important at the temperatures and densities of our study. This can be appreciated by the observation that the phase diagrams of  $^3\text{He}$  and  $^4\text{He}$  on graphite (Fig. 1) are very similar.

We will demonstrate that the phases of  $^3\text{He}$  adsorbed on graphite can be accurately simulated by the Feynman path-integral Monte Carlo method, realistic potential functions for the substrate-adsorbate and adsorbate-adsorbate interactions, and a three-dimensional geometry. The fluid, commensurate solid, incommensurate solid, and reentrant fluid ( $\beta$ ) phases are found and are in agreement with the experimental phase diagram. The microscopic structure of the reentrant fluid is observed to be a striped domain-wall liquid, in agreement with the

experimental interpretation of Motteler<sup>4</sup> and the striped helical Potts model calculation of Halpin-Healy and Kardar.<sup>6</sup> Only after our simulation of the *fluid* in the  $\beta$ -phase region were we made aware of the fact that it had been suggested earlier.<sup>7</sup>

In the Feynman path-integral representation, a single quantum particle is isomorphic to a classical cyclic polymer chain of  $M$  beads in which each bead  $j$  interacts with its neighboring beads  $j-1$  and  $j+1$  through a harmonic force constant  $mM/\hbar^2\beta^2$  and experiences a reduced external potential  $V(\mathbf{r}(j))/M$  (the particle mass is  $m$ , and  $\beta$  is inverse temperature). The harmonic coupling arises from the free-particle propagator  $f$  describing the quantum-mechanical contribution of kinetic en-

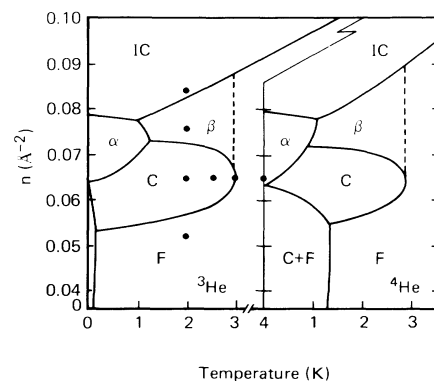


FIG. 1. Phase diagrams for  $^3\text{He}$  and  $^4\text{He}$  on graphite from Ref. 1. The  $\beta$  phases were not a part of the original published diagrams and were taken from Ref. 4. The solid circles denote temperature-density locations where the Monte Carlo simulations were performed.

ergy to the density matrix,

$$f(\mathbf{r}(j+1), \mathbf{r}(j); \beta/M, L) \equiv (Mm/2\pi\beta\hbar^2)^{3/2} \sum_n \exp\{- (Mm/2\beta\hbar^2)[\mathbf{r}(j+1) - \mathbf{r}(j) - nL]^2\}. \quad (1)$$

This representation is exact only in the limit of  $M$  going to infinity. For a given temperature and density, one has to determine empirically the value of  $M$  beyond which the thermodynamic properties do not effectively change. The lower the temperature, the larger  $M$  must be. We have adopted a higher-order correction to this "high-temperature approximation." It takes the form<sup>8</sup> of a simple modification to the potential energy  $V$ :

$$V'(\mathbf{r}(j)) = V(\mathbf{r}(j)) + \frac{1}{24} \frac{\hbar^2}{m} \left( \frac{\beta}{M} \right)^2 \left( \frac{\partial V}{\partial \mathbf{r}(j)} \right)^2. \quad (2)$$

We refer the reader to the papers of Takahashi and Imada<sup>8-10</sup> for a detailed description of the path-integral Monte Carlo method that we implemented. Unless the <sup>3</sup>He atoms were treated as distinguishable, direct calculation of the determinant of free-particle propagators was performed in the evaluation of the Monte Carlo weight function  $|W|$  for the spinless fermion system of  $N$  atoms,<sup>11</sup>

$$W = (N!)^{-M} \prod_{j=1}^M \det A(j+1, j) \exp \left[ - \frac{\beta}{M} \sum_{j=1}^M V'(j) \right], \quad (3)$$

and

$$\{A(j+1)\}_{k,l} = f(\mathbf{r}_k(j+1), \mathbf{r}_l(j)), \quad 1 \leq k, l \leq N, \quad (4)$$

where  $V'(j) = V'(\mathbf{r}_1(j), \dots, \mathbf{r}_N(j))$  is defined by Eq. (2), and  $A(j+1, j)$  is an  $N \times N$  matrix of the one-particle-propagator matrix elements  $f(\mathbf{r}_k(j+1), \mathbf{r}_l(j))$ . The absolute value of  $W$  is taken since the weight function in importance sampling should be positive. Two kinds of displacements of coordinates are adopted for importance sampling; a "microscopic" displacement of an individual bead and a "macroscopic" displacement of all of the beads in a cyclic polymer chain according to the recipe of Takahashi and Imada.<sup>9</sup> One Monte Carlo move is defined as  $N$  attempted macroscopic displacements, each one made after  $M$  trials of the microscopic displacements. Primitive displacement parameters were adjusted so that the acceptance ratios for microscopic and macroscopic displacements are approximately one-half. A similar approach for bosons would be impractical since the determinant in Eq. (3) becomes a permanent, and one must approach the boson problem in a different manner.<sup>4</sup>

In our Monte Carlo simulations, the number of atoms varied from 36 to 42, depending on the coverage of interest, chosen dimensions of the graphite substrate, and compatibility with periodic conditions for the initialized triangular lattice of a helium solid and the graphite lattice. Periodic boundary conditions were imposed at the four faces of the computational cell which pass through

the sides of the basal plane at normal incidence to the surface. A reflecting wall was placed at the top of the computational box beyond the second layer height, but no atom was promoted to the second layer in any of the simulations. We adopted the Lennard-Jones 12-6 pair potential to represent the interaction between helium atoms and between helium and carbon atoms, and the potential parameters are taken from Cole and Klein.<sup>12</sup> Similar parameters have been shown to describe the phase diagram of classical rare-gas atoms on graphite very well.<sup>13</sup> The graphite was modeled as a semi-infinite rigid solid.

By experimentation, we found that 96 beads are required to obtain energy convergence at 2.0 K, and we used bead numbers of 84, 72, and 48 for temperatures of 2.5, 3.0, and 4.0 K, respectively. We also learned that fermion exchange is unimportant for temperatures equal to and above 2.0 K for the coverages of our study.<sup>14</sup> Perhaps this is due to the two-dimensional nature of the system. For example, <sup>4</sup>He films have no momentum condensate.<sup>15</sup> In Fig. 1, the solid circles denote temperature-density locations where the Monte Carlo simulations were performed. Equilibrium was determined by

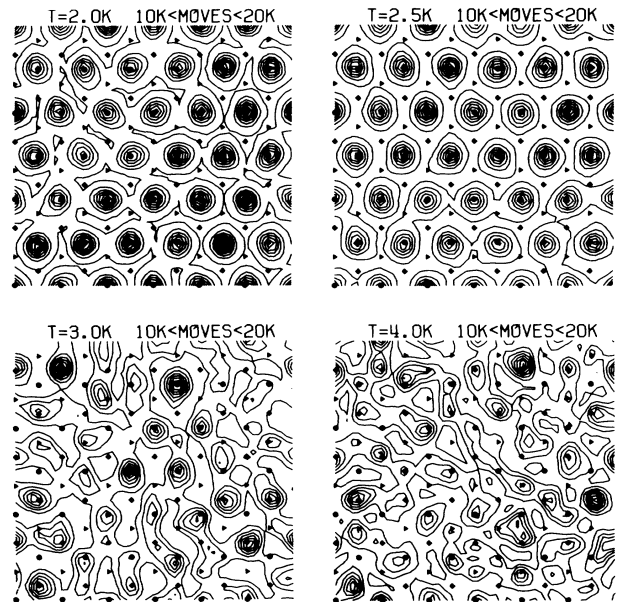


FIG. 2. The probability density contours for the helium beads averaged over 10 000 Monte Carlo moves. The coverage is unity, and the temperatures are 2.0, 2.5, 3.0, and 4.0 K. The solid circles, triangles, and lozenges denote the threefold energetically degenerate adsorption sites on graphite for a commensurate solid.

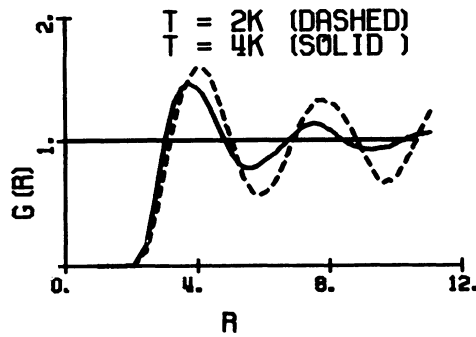


FIG. 3. The helium radial distribution functions for the commensurate solid at 2.0 K and for the fluid coverage of unity at 4.0 K.

monitoring of the energies and structural distribution functions for a given simulation. In Fig. 2, the probability density contour plots for the helium beads are presented for a coverage of unity and for temperatures of 2.0, 2.5, 3.0, and 4.0 K, respectively. The distribution was obtained by our averaging over 10000 Monte Carlo moves after at least 10000 previous moves were made from the initialized triangular lattice. The averaging interval is given above each part. As a consequence of the size of the helium atom, only one-third of the adsorption sites can be occupied by a commensurate solid, and there exist three energetically degenerate commensurate sub-

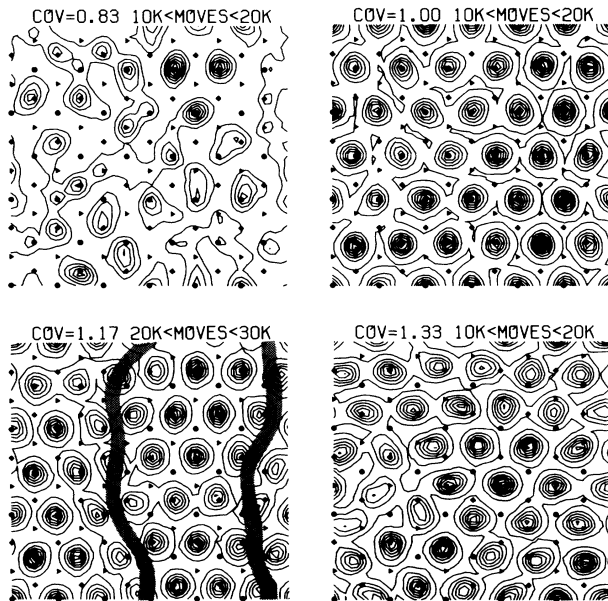


FIG. 4. The probability density contours for the helium beads averaged over 10000 Monte Carlo moves. The temperature is 2.0 K, and the coverages are 0.83, 1.00, 1.17, and 1.33. The shaded stripes pictorially denote the striped domain walls. See Fig. 2 for additional details.

lattices. The solid circles, triangles, and lozenges denote these commensurate sublattices. We see that the commensurate solid state exists at 2.0 and at 2.5 K and that the fluid state exists at 3.0 and 4.0 K, in agreement with experiment (Fig. 1). The radial distribution functions for the commensurate solid at 2.0 K and for the fluid at 4.0 K are presented in Fig. 3. In Fig. 4, the probability density contour plots for the helium beads are presented for the temperature of 2.0 K and the coverages of 0.83, 1.00, 1.17, and 1.33. We see the low-density fluid, commensurate solid, high-density reentrant fluid, and high-density incommensurate solid as we pass from low to high coverage, and these phases appear to be in agreement with the experimental phase diagram (Fig. 1). In particular, the microscopic structure of the reentrant fluid is observed to be a striped domain-wall liquid, in agreement with the experimental interpretation of Motzler<sup>4</sup> and the striped helical Potts model calculation of Halpin-Healy and Kardar.<sup>6</sup> The shaded stripes pictorially denote the striped domain walls. The wall thickness is approximately one to two helium atomic diameters and is consistent with the prediction of theory.<sup>6</sup>

Table I gives the total, potential, and kinetic energies for our constant-coverage and constant-temperature cuts through the phase diagram. For the commensurate-density simulations, the potential and kinetic energies increase as the fluid phase is entered, the potential-energy change being larger. For the constant-temperature simulations, the potential energy decreases and the kinetic energy increases with increasing coverage. The kinetic energy increase due to compression is quite dramatic. As defined by Schoebinger and Abraham,<sup>16</sup> the domain-wall energy per unit length is estimated to be approximately unity, but an analysis like the study in Ref. 16 is not presently feasible. The exploration of the helium-graphite phase diagram is seen to be a subtle balance of competing energetic effects, and it is gratifying that the

TABLE I. Total energy ( $E_{tot}$ ), potential energy ( $E_{pot}$ ), and kinetic energy ( $E_{kin}$ ) per atom for constant-commensurate-density simulations as a function of temperature  $T$  and for constant-temperature simulations ( $T=2$  K) as a function of coverage  $\theta$ . Energy unit is  $10^{-13}$  ergs/atom, and the statistical uncertainty of the measured energies is in the fourth decimal point.

	$E_{tot}$	$E_{pot}$	$E_{kin}$
$T=2.0$ K	-0.1846	-0.2347	0.0500
$T=2.5$ K	-0.1842	-0.2347	0.0504
$T=3.0$ K	-0.1819	-0.2328	0.0510
$T=4.0$ K	-0.1818	-0.2330	0.0512
$\theta=0.83$	-0.1844	-0.2302	0.0457
$\theta=1.00$	-0.1846	-0.2347	0.0500
$\theta=1.17$	-0.1809	-0.2361	0.0552
$\theta=1.33$	-0.1766	-0.2377	0.0611

simulations agree so well with laboratory experiment.

It is essential to treat much larger-size systems in order to achieve the needed detail required for a quantitative analysis. In particular, the microscopic structure and energetics of the domain-wall network are needed. Also, lower-temperature simulations will allow a thorough examination of the phase diagram; e.g., the  $\alpha$  phase. We are presently implementing the matrix-squaring method<sup>4</sup> requiring fewer beads and algorithms amenable to parallel computation in hopes that we can approach systems of a thousand atoms using a special-purpose array computer (see Ref. 13, Sec. 4.2).

The work has benefited greatly from discussions with John Barker, IBM Almaden Research Center. One of the authors (F.F.A.) is indebted to Professor Sam Fain and Professor Greg Dash, University of Washington, for valuable discussions and advice. One of us (J.Q.B.) would like to thank the U.S. Department of Energy for its generous support under Grant No. DE-FG02-85ER45218.

---

<sup>1</sup>M. Schick, in *Phase Transitions in Surface Films*, edited by J. G. Dash and J. Ruvalds (Plenum, New York, 1980), p. 68. For a more recent experimental study, the reader is referred to R. E. Ecke and J. G. Dash, *Phys. Rev. B* **28**, 3738 (1983).

<sup>2</sup>B. J. Alder, D. M. Ceperley, and E. L. Pollock, *Acc. Chem. Res.* **18**, 268 (1985).

<sup>3</sup>D. M. Ceperley and B. J. Alder, *Science* **231**, 555 (1986).

<sup>4</sup>F. C. Motteler, Ph.D. dissertation, University of Washington, Seattle, WA, 1986 (unpublished).

<sup>5</sup>D. M. Ceperley and E. L. Pollock, *Phys. Rev. Lett.* **56**, 351 (1986).

<sup>6</sup>T. Halpin-Healy and M. Kardar, *Phys. Rev. B* **34**, 318 (1986). For Kr on graphite, the domain-wall liquid was first suggested theoretically by S. N. Coppersmith, D. S. Fisher, B. I. Halperin, P. A. Lee, and W. F. Brinkman, *Phys. Rev. B* **25**, 349 (1982).

<sup>7</sup>S. C. Fain, private communication. One of the authors (F.F.A.) is indebted to Professor Fain for pointing out that we were possibly simulating a domain-wall liquid and for bringing Refs. 5 and 6 to his attention.

<sup>8</sup>M. Takahashi and M. Imada, *J. Phys. Soc. Jpn.* **53**, 3765 (1984).

<sup>9</sup>M. Takahashi and M. Imada, *J. Phys. Soc. Jpn.* **53**, 963 (1984).

<sup>10</sup>M. Imada and M. Takahashi, *J. Phys. Soc. Jpn.* **53**, 3770 (1984).

<sup>11</sup>In Ref. 9, it is stated that the determinant evaluation scales as the cube of the number of particles. However, in the Monte Carlo procedure, only one row is changed for an attempted displacement, and an algorithm for the determinant evaluation has been devised that scales as the square of the number of particles (Nimrod Megiddo, private communication).

<sup>12</sup>M. W. Cole and J. R. Klein, *Surf. Sci.* **124**, 547 (1983).

<sup>13</sup>F. F. Abraham, *Adv. Phys.* **35**, 1 (1986).

<sup>14</sup>The details of convergence, exchange, and energetics will be described in an expanded publication.

<sup>15</sup>J. G. Dash, *Phys. Rep.* **38C**, 177 (1978).

<sup>16</sup>M. Schoebinger and F. F. Abraham, *Phys. Rev. B* **31**, 4590 (1985).